C5-1471.7/3111 Copy 5

PROCESS TECHNIQUES STUDY OF INTEGRATED CIRCUITS

Quarterly Report No. 7

February 1967

Prepared by:

J. E. Meinhard

AUTONETICS
A DIVISION OF NORTH AMERICAN AVIATION, INC.
Prepared Under Contract

NAS 12-4

General Order 6433

Approved by:

P. H. Eisenberg
Supervisor
Special Projects Unit
Materials and Processes Laboratories

Approved by:

H. C. Mattraw
Assistant Director
Physical Sciences
Research and Engineering

PROCESS TECHNIQUES STUDY OF INTEGRATED CIRCUITS

Quarterly Report No. 7

ABSTRACT

The objective of present work is to obtain more quantitative information on the entrapment of hydrogen in grown silicon dioxide layers using tritium as a tracer and to seek evidence of its possible ionic mobility in a potential gradient. Other objectives include the interpretation of the EPR second signal as a possible indicator of oxygen vacancies, the investigation of gas embient effects on integrated circuits, and the elucidation of the machanics and dynamics of structural defects in oxide layers.

Analysis of wafers from recent tritium experiments duplicating the conditions reported by Burgess and Fowkes has failed to show any measurable beta activity. The differences between results obtained on this program and those of Burkhardt, and of Burgess and Fowkes, are summarized and explained.

An initial attempt to demonstrate proton electromigration in thermal oxide has not produced a measurable result.

Thirty integrated circuits selected from three manufacturers have been electrically characterized and the contained package ambients analyzed by mass spectrometry. Little variation in initial electrical parameters was found, but gas ambient compositions varied widely. The output transistors of these IC's have been rebonded to permit beta measurements. An environmental chamber of extended range is being fabricated for the further investigation of these devices.

Evidence from EPR absorption spectrometry of thermally grown oxides indicates that the presence of unpaired electron spins may be associated with prior HF treatments such as those used in chemical polishing of wafers or in window etching.

EPR absorption of an aluminized oxide on silicon has yielded a peak with a g value of 2.0023 ± 0.0004. No impurities in excess of one per cent by weight was found in these samples by microprobe analysis.

A correlation of better than 99 per cent has been found between dielectric defect incidence and wafer cooling after exposure to vapor phase etching. This result is considered to provide the first direct evidence that film rupture is due to the thermal contraction difference between silicon and silicon dioxide as earlier proposed.

Evidence has been obtained which indicates that removal of the oxide layer from one side of a wafer causes structural damage to the oxide on the other side. Dielectric defects appear to be restricted to regions of the oxide in which some blemish or structural variation is evident.

Evidence from another set of experiments indicates that oxide defects are not in any way related to dislocation densities or stacking fault densities in the substrate silicon.

PROCESS TECHNIQUES STUDY OF INTEGRATED CIRCUITS

Quarterly Report No. 7

ACCOMPLISHMENTS

A. Oxide Radiotracer Experiments

New tritium experiments were conducted at the General Atomic facilities. Three runs were performed, one of which duplicates the conditions reported by Burgess and Fowkes[1]. A total of seventy-five wafers were treated, and representative samples from each run were prepared for analysis by stripping off the back oxide layer to allow grounding to the counting chamber and prevent beta attenuation by positive charge accumulation. The experiment duplicating the Burgess and Fowkes conditions utilized a gas phase composition corresponding to air (0.2 atm O_2) and a specific activity of 0.1 mc/g in the injected water. The other two experiments were conducted in a 50/50 O_2/N_2 ambient carrying tritiated water of 10 mc/g specific activity. The main difference between the last two experiments was the water reservoir temperature: 36 C and 94 C, respectively. Precise determinations of the gas phase water content in all three runs were obtained from the carrier gas flow rates and the condensed water mass differences in the exit cold trap. All three runs failed to yield wafer specimens with a detectable beta activity.

In view of our earlier results, and of those obtained by Burkhardt[2], the levels reported by Burgess and Fowkes (10^{20} H atoms/cm^3 oxide) seem highly improbable. This conclusion is clearly indicated by summarizing the various experimental conditions and computing the actual activity levels present in each case, as shown in Table I. In this table runs 3, 4 and 5 are the experiments recently conducted on this program (December 9 to 13, 1966), and runs 1 and 2 are earlier experiments (September 15, 1965, and

TABLE I. COMPARISON OF TRITIUM DIFFUSED SILICON OXIDATION CONDITIONS

RUN	T_2O SOURCE ACTIVITY (mc/g)	SYSTEM	CARRIER GAS COMPOSITION (P_o atm) O_2	H_2O	GAS PHASE SPECIFIC ACTIVITY (CURIE atm X 10^3)	COMPUTED H CONTENT (ATOMS/cm^3)	COUNTING METHOD	TRITIUM REFERENCE STANDARD
3*	0.1	Flow	0.2	0.011	0.0011	(0)	Methane Proportional	Polymethyl-methacrylate**
4*	10	Flow	0.5	0.039	0.39	(0)	"	"
5*	10	Flow	0.5	0.045	0.45	(0)	"	"
1*	1	Semi-Static	0.5	0.09***	0.9	$\sim 3 \times 10^{15}$	"	"
2*	1000	Static	0.5	0.1	100	$\sim 2 \times 10^{16}$	"	"
Burkhardt	500	Static	-0-	1.0	500	$\sim 10^{20}$	Liquid Scintillation	T_2O Standard**
Burgess & Fowkes	0.1	Flow	0.2	0.01***	0.001***	$\sim 10^{17}$	Not Reported	Not Reported

*Performed on Contract NAS 12-4

**Supplied by New England Nuclear Corp.

***Estimated

October 7, 1965, respectively.) Estimated activity levels in the Burgess and Fowkes experiment are based on available evidence from their report[1] and our duplication of their conditions in run 3. It is not conceivable that the gas phase specific activity in their experiment could be more than a factor of 10^{-5} those of Burhardt and of our run 2. Additionally our run 1 at 10^3 times the activity of the Burgess and Fowkes experiment gave specimens of barely perceptible beta activity (see Fifth Monthly Report, September, 1965) and our runs 4 and 5 at slightly lower tritium levels gave no detectable results. It must be concluded that the Burgess and Fowkes result is unacceptable pending more detailed evidence from that laboratory.

Confidence can be placed in the Burkhardt result, however, because of the considerable care exercised in standardizing experimental conditions and counting technique. Liquid scintillation counting, although generally regarded as more sensitive, offers no advantage in accuracy over our methane proportional counting because both techniques were calibrated against reference standards from the same source (New England Nuclear Corp.). The difference in results lies rather in the use of pure tritiated steam as the oxygen source in the Burkhardt experiment whereas in our run 2 the steam represented only 0.1 the total available oxygen. Moreover, the Burkhardt oxidation was carried out close to the glass transition temperature (1000 C), where out-diffusion of hydrogen is less rapid, and no provision was available for subsequent flushing and desorption of adsorbed species at the oxidation temperature. In run 2 the oxidation (at 1150 C) was followed by a thorough tracer-free nitrogen purge. All of the above conditions specified for the Burkhardt experiment tend to maximize hydrogen entrapment and represent a significant departure from normal processing technology. Our experiments show that as more conventional conditions are approached the hydrogen retention in the oxide, although still demonstrable, is significantly reduced.

The data of Burkhardt[2] indicate that oxide attenuation of recoverable beta activity is a substantially larger effect than originally anticipated. Space charge effects within the insulating layer are suspected as

the major contributing factor (see below) because the calculated average range of 18 Kev beta particles in SiO_2 is about 13,000 Å (quarterly Report No. 1, August, 1965), and the maximum range, 40,000 Å. The magnitude of the error introduced by this effect can be determined experimentally by stepwise etching and counting. Although this should lead to higher results for our earlier investigations, an increase by a factor of 10^3 or better, is not foreseeable.

It should be pointed out that the foregoing arguments relate only to the quantitative aspects of the previous runs and have no direct bearing on the success in fulfilling the original qualitative intent of these experiments.

The possibility that the insulating properties of silicon dioxide layers may influence 4-pi beta assay procedures for tritium estimation was first suggested in the twelfth monthly report (April, 1966). Although the beta energies involved (18 Kev) substantially exceeded the attenuation in the oxide layers, the 4-pi technique did not prevent build-up of a compensating positive charge in the silicon substrate which could trap and retain a portion of the beta emission. A test of this possibility was undertaken as described in the thirteenth monthly report (May, 1966) by exposing one side of the wafer surface and bonding a gold contact thereto. The specimen, which now provided essentially 2-pi geometry, was assayed for beta activity with the results given in TABLE II.

TABLE II. EVALUATION OF GROUNDED COUNTING TECHNIQUE

SPECIMEN NO.	ORIGINAL BETA COUNT (Min^{-1})	DATE	CALCULATED H CONTENT* ($atoms/cm^3$)	GROUNDED COUNT (Min^{-1})	DATE	CALCULATED H CONTENT* ($atoms/cm^3$)	TECHNIQUE FACTOR
6	246	3/22/66	2.65×10^{16}	518	11/3/66	5.73×10^{16}	2.17

*Corrected to date of original tracer experiment (10/7/65).

The factor of 2.17 given in TABLE II is strong evidence of positive charge accumulation in the silicon wafer when insulated by both oxide layers. Since this factor is not corrected for beta attenuation or space charge effects, as suggested above, in the remaining oxide layer or for possible environmental exchange (estimated at $\sim$ 20 percent over one year) the average hydrogen content of this oxide actually may be in the range of 10^{17} $atoms/cm^3$. This value

still is substantially less than the 10^{20} atoms/cm^3 reported elsewhere and analyzed above.

Electromigration of tritium in oxide layers was attempted at 200 C and a bias of 150 V using aluminum foil plates in contact with the oxide, as described in the thirteenth monthly report (May, 1966). The beta activity remaining in the oxide after this treatment was not significantly different from the original activity, indicating either that the hydrogen was immobile under the experimental conditions or that the foil electrodes were not in sufficiently intimate contact with the oxide to permit cathodic deposition. Burkhardt's attempt to demonstrate hydrogen electromigration[2] also yielded a negative result and the transport of positive charge may be dependent on a proton-sodium ion exchange. The possibility of such exchange was suggested in the original proposal for this investigation. In spite of these initial negative results the independent electromigration of hydrogen ions in thermal oxide cannot be regarded as a refuted possibility.

B. GAS AMBIENT EFFECTS

Thirty general purpose amplifier integrated circuits (ten each from Texas Instruments, Westinghouse and Norden) have been selected to investigate the effects of ambient hydrogen on transistor gains. The test program will proceed in the following steps:

1. Selection of samples
2. Electrical characterization
3. Mass spectrographic analysis of package ambients
4. Measure output transistor beta
5. Vacuum bake
6. Measure output transistor beta
7. Bake in forming gas
8. Measure output transistor beta
9. Vacuum bake
10. Measure output transistor beta
11. Correlate data

The thirty integrated circuits have been electrically characterized and the data given in TABLE III & TABLE IV. The parameters measured for are the following:

Sample No.	Vendor	Type No.	TEST NUMBER AND TYPICAL LIMITS 1	2	3	4	5	5	6	7	8	9	9
			7.5 MV DC	350 MV DC	170 to 245	Unit-less	More Than 8.75 Vac.	More Than 8.75 Vac.	MV	Unit-less	Unit-less, x10^{-4}	3.4 to 9.0 ma I(+6)	3.4 to 10 ma I(-12)
6	TI	0940	3.9	290	194	0.96	10.70	10.66	4.9	171	4	5.48	5.92
7	TI	0940	1.0	190	183	0.92	10.79	10.79	2.5	154	9	5.56	5.99
8	TI	0940	2.5	195	192	0.94	10.78	10.75	5.2	149	2	6.44	6.94
9	TI	0940	7.0	264	193	0.94	10.77	10.74	8.3	159	2	6.11	6.53
10	TI	0940	2.4	272	194	0.97	10.76	10.74	3.3	158	18	6.52	7.03
11	W	0940	4.1	21	180	0.88	10.11	10.03	6.2	159	1	5.78	6.29
12	W	0940	6.8	91	183	0.91	10.01	9.98	116	148	4	6.04	6.56
13	W	0940	1.1	5	184	0.90	10.00	9.91	1.9	155	1	6.55	7.12
14	W	0940	1.7	146	188	0.91	10.48	10.47	0.4	146	14	6.29	6.82
15	W	0940	0.2	24	176	0.87	9.83	9.70	0.0	126	0	5.98	6.49
21	N	0940	2.8	54	187	0.89	10.58	10.61	1.7	135	6	7.25	7.86
22	N	0940	3.1	19	183	0.93	10.62	10.64	3.2	169	4	5.54	6.03
23	N	0940	1.2	134	189	0.96	10.68	10.68	1.3	146	0	6.33	6.87
24	N	0940	1.6	168	194	0.94	10.77	10.74	1.9	150	9	6.05	6.55
25	N	0940	0.2	54	191	0.94	10.73	10.70	1.8	146	5	6.43	6.97

TI - Texas Instruments
W - Westinghouse
N - Nordec

TABLE III - INITIAL ELECTRICAL DATA ON 0940 ICS

Sample No.	Vendor	Type No. MD 477-	TEST NUMBER AND TYPICAL LIMITS 1 14 MV DC	2 700 MV DC	3 2000 to 8000	4 Unit-less	5 More Than 8.75 Vac.	5 More Than 8.75 Vac.	6 MV	7 Unit-less	8 Unit-less	9 4 to 11 ma I(+6)	9 0.7 to 2.2 ma I(+12)	9 3.5 to 10 ma I(-12)
1	TI	0947	1.3	0.1	3395	1.76	11.20	11.09	7.5	2779	15	4.41	1.03	5.81
2	TI	0947	4.3	37	2808	1.42	11.03	10.92	8.5	2544	10	4.85	1.20	6.43
3	TI	0947	8.2	461	2866	1.44	11.07	11.12	14.5	2140	11	5.73	1.19	7.39
4	TI	0947	1.5	283	2702	1.43	10.99	11.06	1.8	2603	11	5.13	1.12	6.84
5	TI	0947	4.6	450	2451	1.24	10.99	10.92	5.6	2039	6	5.42	1.14	6.99
16	W	0947	2.3	400	3615	1.84	11.05	10.85	3.2	2970	29	6.39	1.29	8.19
17	W	0947	1.9	458	2210	1.13	10.73	10.85	1.7	1724	14	5.85	1.14	7.46
18	W	0947	1.8	140	2092	1.05	11.11	10.94	4.8	1459	8	6.00	1.20	7.88
19	W	0947	1.8	264	3084	1.57	10.93	10.89	1.8	2486	12	6.05	1.19	7.76
20	W	0947	1.5	393	3565	1.81	10.64	10.75	1.6	2987	15	5.78	1.19	7.43
26	W	0947	0.5	322	2587	1.30	11.01	10.96	0.5	2300	10	5.11	1.27	6.85
27	W	0947	2.1	424	3471	1.73	10.95	10.94	3.4	2886	12	5.67	1.44	7.66
28	W	0947	2.2	247	4062	2.03	11.04	10.96	0.7	3625	15	5.54	1.34	7.38
29	W	0947	1.6	340	2527	1.27	10.99	10.96	0.6	2222	13	5.32	1.32	7.14
30	W	0947	2.1	281	2902	1.44	11.10	11.02	0.7	2562	14	5.64	1.38	7.56

TI - Texas Instruments
W - Westinghouse
N - Norden

TABLE IV - TYPICAL ELECTRICAL DATA ON 0947 ICs.

Test 1. Differential DC Input Voltage Offset (DIVO)

Test 2. Common Mode DC Output Voltage Offset (CMOVO)

Test 3. Low Frequency AC Voltage Gain (GV)

Test 4. Single Ended Low Frequency AC Voltage Gain (GV^1)

Test 5. AC Signal Swing (two leads) (ACSS)

Test 6. Differential DC Current Offset (DICO)

Test 7. Input Impedance (Z in)

Test 8. Midband Common Mode Rejection Ratio (CMRR)

Test 9. Power Supply Currents (Three voltages)

The data provided by these tests, which are part of the Autonetics specifications NA5-16071 for the IID 477-0940 GPA and NA5-16078 for the IID 477-0947, will be correlated with the subsequent data to be generated. Three of the significant parameters are not measured experimentally but may be calculated from:

$$Z \text{ in} = \frac{RS}{\left(\frac{\text{Test 3}}{\text{Test 7}} - 1\right)} \qquad (1)$$

$$CMRR = 20 \text{ Log}_{10} \left(\frac{10^2 \times \text{test 4}}{\text{test 8}}\right) \qquad (2)$$

$$DICO = \frac{\text{test 6} - \text{test 1}}{RS} \qquad (3)$$

Where RS = 30,000 ohms for the 940

RS = 3,000 ohms for the 947

Twenty of these integrated circuits were selected for gas analysis on a mass spectrometer. The results are shown in TABLE V, and indicate extensive device-to-device variations in gas composition. The major constituent in the TI devices (samples 2-9) was nitrogen, the desired package ambient. However, four devices contained He and five devices contained small amounts of CO_2. The large amount of He present evidently originated from pressurizing the devices in helium prior to leak testing somewhere in the device history. The CO_2 trace could be present as impurities in the N_2 dry box gas.

The Norden devices (samples 21-30) also show the major constituent as N_2 with traces of O_2, CO_2, and A in some packages. Device 30, however, contained 44.6 percent N_2, 9.5 percent O_2, 44.5 percent He, 0.9 percent CO_2, and 0.5 percent A. This indicates that this device had a package with a high leak rate, thus allowing air to leak into the package over a period of

VOLUME PERCENT GAS IN INTEGRATED CIRCUIT PACKAGE

Sample	Vendor	Type	N_2	O_2	He	CO_2	A	H_2	CH_4	Volume Atm. (Microliter)
2	TI	947	[illegible]	0.3	3.7	0.7				6.01
4	TI	947	97.3		2.3	[illegible]				7.44
5	TI	947	92.[illegible]		[illegible].7	[illegible].9				[illegible].05
7	TI	940	72.7		20.9	0.3	0.1			8.37
8	TI	940	100							8.05
9	TI	940	99.6			0.4				7.97
11	W	940	7.8	0.8				91.4		3.31
12	W	940	56.9	40.7		1.2	1.2			1.07
15	W	940	(Leaker)							
17	W	947	5.5			0.2	0.4	93.9		3.99
18	W	947	72.1	19.2	7.6	0.2	0.9	7.6		6.42
19	W	947	12.4	2.0				[illegible].2	0.2	3.06
21	N	940	99.1	0.9						1.94
22	N	940	99.6			0.2	0.2			3.21
23	N	940	100							1.86
24	N	940	98.8	0.1		0.4	0.4			1.44
26	N	947	99.6			1.2				2.92
28	N	947	99.6			0.4				3.01
29	N	947	99.5			0.5				2.47
30	N	947	84.6	10.0	4.5	0.9	0.5			6.49

TI - Texas Instruments
W - Westinghouse
N - Norden

TABLE V MASS SPECTROMETER DATA OF PACKAGE AMBIENTS

time. The gas volume noted also indicated a leaky package as the Norden package is sealed at a high temperature and thus upon cooling a partial vacuum should exist inside the package. The extremely large gas volume of device 30 relative to the other Norden devices indicates that in-leakage of external air equalized the pressure.

The Westinghouse devices (samples 11-19) showed the most erratic behavior in terms of gas composition. Three devices, (11, 17, and 19) showed H_2 contents above 85 percent with a smaller percentage of N_2. Two devices (12 and 18) showed major amounts of N_2 and O_2 and no detectable H_2. An explanation of the package sealing technique will be necessary in order to explain this effect. The devices are braze sealed in a continuous-belt furnace which has a nitrogen blanket on both ends and a small region of H_2 at the center of the furnace. Therefore, the package ambient composition will depend on the position in the furnace at which the package is actually sealed via a brazing alloy. This would indicate that the devices containing the hydrogen (11, 17, and 19) were sealed in the center of the furnace.

The presence of O_2 in devices 12 and 18 is more difficult to explain, especially since hermeticity tests were not performed immediately prior to gas analysis. However, it would appear that these two devices were hermetic seal leakers, which allowed the H_2 present to escape and allowed the composition to equilibrate with external air. The presence of more than the air percentage of O_2 in device 12 cannot be explained at this time.

The output transistors of these integrated circuits have been rebonded to permit beta measurements at various base currents. Modification of a vacuum chamber is being performed to provide 10^{-6} Torr pressure and temperatures to 250 C for step 5 of this investigation.

C. EPR SPECTROMETRY

Additional EPR data on samples (M^1W + HF), (M^1 + NaCl) and (TW) have been obtained. Of particular interest are the results on sample (M^1W + HF) under atmospheric and reduced pressures shown in Figure 1. It is evident from the figure that outgassing of the HF treated sample (at 4×10^{-2} Torr) produces a significant reduction in the second signal. The second signals of the other two samples, however, were unresponsive to outgassing. The evidence appears to implicate the HF + Si system as a source

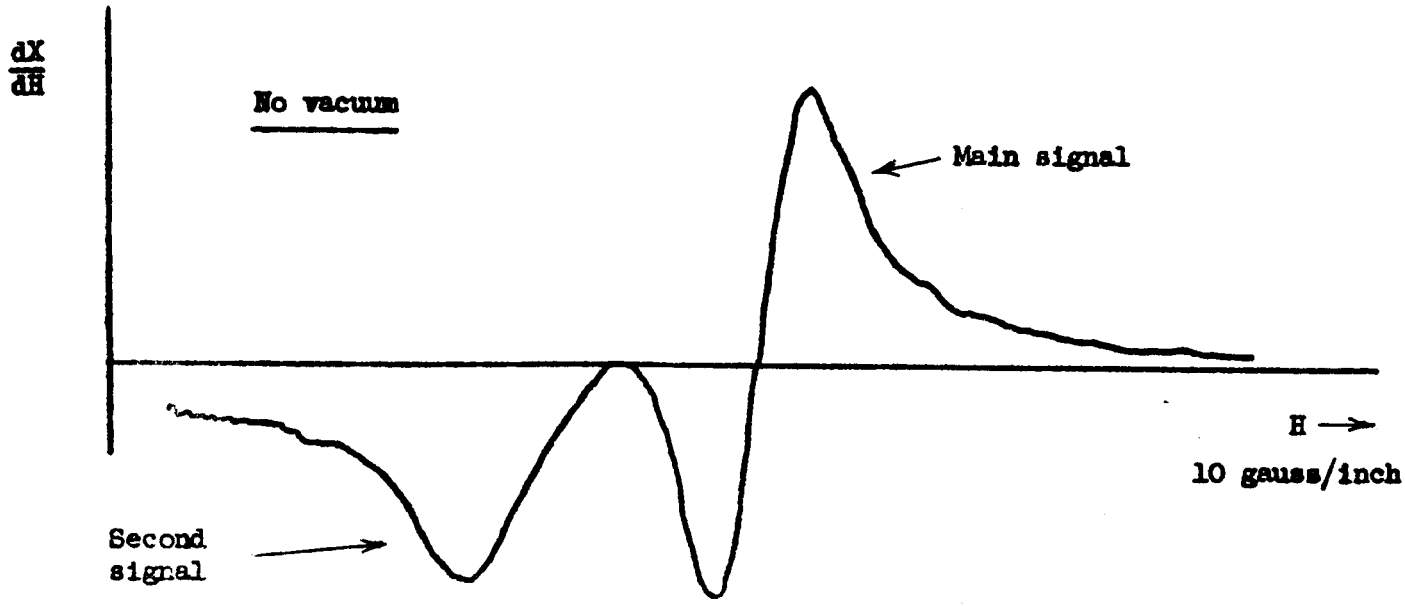

gain = 1000
modulation = 1000
response = 1 second
temperature = -184C

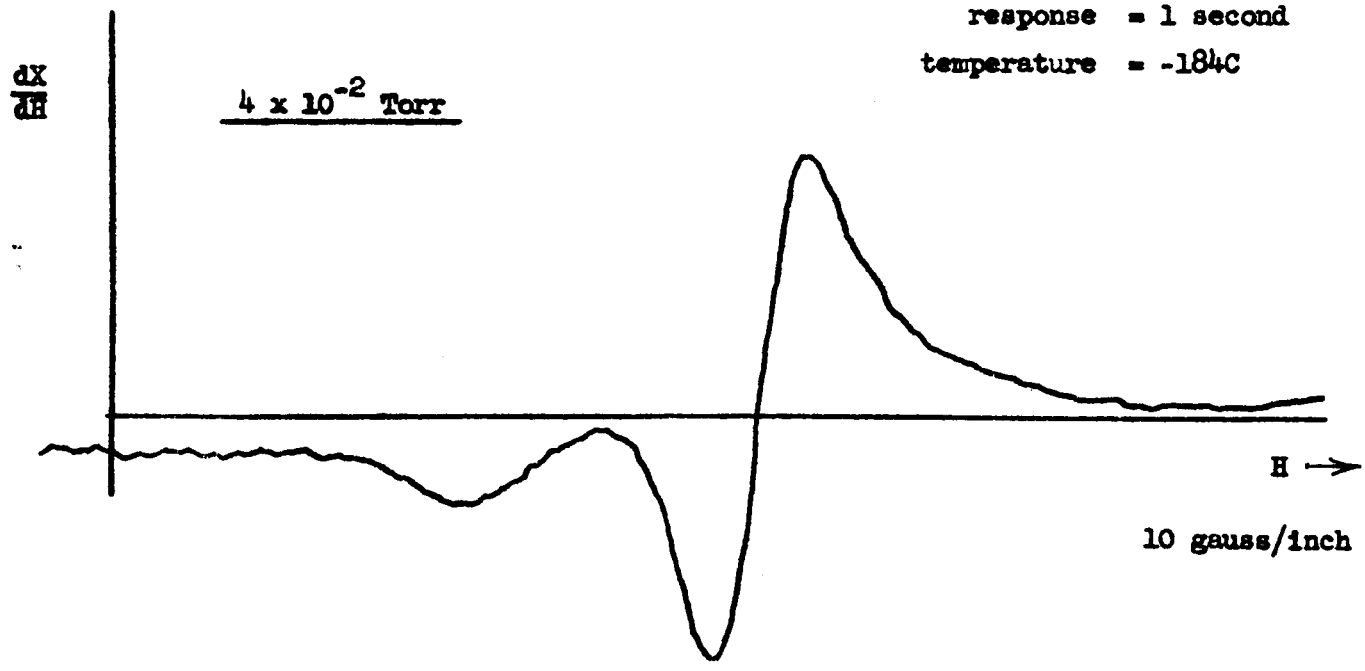

Figure 1. Sample ($M^{1}W$ + HF)

of the second signal. It is known, for example, that SiF_4 (formed in the present experiment by HF + SiO_2) interacts with silicon at elevated temperatures to produce the biradical Si_2F_4 containing unfilled silicon orbitals. However, the reverse of this reaction at still higher temperatures should result in release of SiF_4 and deposition of "atomic" or finely divided silicon. This possibility fits well with the experimental conditions employed because the specimen (M^1W + HF) was baked for ten minutes at 1150 C in an inert atmosphere after treatment with 0.5 percent HF solution. The residual finely divided silicon then could act as adsorption sites for condensable gases during EPR Spectrometry. This also is a real possibility because the EPR Spectra were taken at -185 C, and the second signal reappeared on admission of room air to the outgassed sample. Although the possibility of residual contamination by fluorinated species cannot be ruled out, the reversibility of outgassing effects on the EPR signal appears to be associated with the sorption of atmospheric components on surfaces rendered sensitive by the HF treatment.

The implications of this finding with respect to integrated circuit processing may be significant because of the extensive utilization of pattern etching with HF followed by diffusions or other high temperature treatments. If the EPR second signal can be associated with positively charged atomic vacancies the present evidence indicates that HF may play a role in causing inversion and that steps should be introduced to remove it after it has served its function.

The independent main signal on silicon powder has been shown[3] to be somewhat sensitive to various ambients and pressures, possibly as a result of residual surface damage. The lack of main signal change in the present sample (also shown in Figure 1) may be due to intact oxide passivation or to prior removal of surface damage by etching. According to earlier evidence it is highly unlikely that this main signal is associated with defects in the oxide structure.

Burkhardt's experiments on the dielectric relaxation of silicon dioxide led him to rule out sodium ions as a source of oxide instability[4] and to postulate an oxygen vacancy generation mechanism based on a reaction of deposited metal with the silicon dioxide. To explore this possibility by

EPR several samples of 8000 Å oxide grown on single crystal silicon (10 ohm-cm, n type) with aluminum dots deposited on them by E-beam evaporation were prepared. Although the sample area was small (2.5 cm x 0.15 cm) the absorption signal was much larger than any recorded previously, including those of bare silicon powder with its much larger surface area. Silicon dioxide samples grown on single crystal silicon without aluminum have previously produced no signal even at high gains. This sample, (TW + Al) S.C., was only run at room temperature and produced only a single signal.

It has been reported[5] that no resonance signals are obtained from aluminum between 4K and 300K unless ferromagnetic impurities are present. The aluminum used here was 99.999 percent and had been analyzed by emission spectrography, showing copper, iron and magnesium present in levels between .001 - .0001 percent. For the iron this represents about 10^{16} spins per cm^3. On a total volume basis the aluminum present in this sample was calculated to have 3×10^{11} spins which is too small to produce a detectable absorption signal with the available equipment. It appears, therefore, that the present signal is derived solely from an interaction between the aluminum deposit and the oxide surface, in substantial agreement with Burhardt's model. The g value of this single signal has been calculated using the dual cavity and found to be 2.0023 ± 0.0004 at -180 C. It does not appear to be temperature dependent. To check for possible trace impurities these samples where analyzed with the electron microprobe. No elements above atomic number four other than aluminum were found on the oxide.

D. INCIDENCE OF DIELECTRIC DEFECTS

The effort on this portion of the program during the past quarter can be classified into three general areas: (I) Substantiation of the model evolved from previous work which postulates that the dominant mechanism of defect formation in oxide films is rupture of the film due to mechanical stress resulting from the thermal expansion mismatch between silicon and silicon oxide. (II) Investigation of process steps which the model predicts to be oxide quality. (III) Search for the source of variations in the oxide structure at which actual or latent defects occur.

Studies in area I have been directed toward determination of the number of defects present in an oxide layer as it exists subsequent to growth but prior to cooling. Comparison of these defects with the number present after removal of the wafer from the furnace provides a direct evaluation of the number of flaws produced by film rupture during cooling.

The decoration test has proved exceptionally suitable for the low temperature, post-cooling detection of oxide defects. In order to delineate the dielectric flaws present in the grown oxide prior to cooling a preferential in situ vapor etch technique was utilized. It has been demonstrated that HCl vapor will attack silicon at elevated temperatures according to reaction (4) but will not appreciably attack the silicon oxide.

$$4HCl + Si \longrightarrow SiCl_4 + 2H_2 \qquad (4)$$

Utilizing this preferential etching characteristic of HCl, the following experiment was performed to determine the relative incidence of inherent (pre-cooling) and stress-produced oxide defects.

Oxides were grown to 8000 Å thicknesses in steam at 1150 C on a group of 10 phosphorus-doped, $\sim$ 10 ohm-cm wafers. After the required oxidation period the steam flow was discontinued and a dry N_2-HCl - dry O_2 mixture was passed through the furnace for 10 minutes, followed by a 40 minute dry N_2 flush. It was anticipated that under the prevailing conditions the HCl vapor would produce etch pits in the Si surface at points where it was not protected by the oxide layer.

After the nitrogen flush, the wafers were removed from the furnace and subjected to the electrophoretic decoration test. The decoration patterns were photographed and the decorations and the oxide removed from the Si wafer. The wafer was then scanned under a microscope at 50-500X magnification to determine the location of possible etch pits for comparison with the decorated defect pattern. This procedure was completed on 8 of the 10 wafers, the others being fractured during test. On seven of these there are no etch pits visible in the Si at the magnifications utilized. On the remaining wafer one possible etch pit was located at a site coincident with a decorated defect. The total number of defects detected by decoration on each wafer is shown below.

WAFER	TOTAL DEFECTS
1	33
2	27
3	15
4	24
5	28
6	18
7	13
8	27
Total	195

The suspected etch pit was observed on wafer No. 6. Careful examination of the site in question by conventional and Nomarsky microscopy suggested that the anomaly was a mound on the silicon surface rather than an etch pit and that the material composing the mound was polycrystalline. A photograph of this site is shown in Figure 2. The dark region near the center is believed to be the original oxide defect. The oxide was stripped with hydroflouric acid and a proficorder trace was made across this region of the wafer. The trace is shown in Figure 3 and verifies that the anomaly was indeed a mound. Electron beam microprobe analysis of the mound revealed only silicon present in detectable quantities. This evidence leads to the hypothesis that in addition to any HCl etching which occurs according to equation (4), further attack occurred by the reaction of H_2O vapor at low concentration levels with the Si substrate[6] according to reactions (5) through (7).

$$Si\ (s) + H_2O\ (g) = SiO\ (g) + H_2\ (g) \qquad (5)$$
$$Si\ (s) + 2H_2O\ (g) = SiO_2\ (s) + 2H_2\ (g) \qquad (6)$$
$$Si\ (s) + SiO_2\ (s) = 2SiO\ (g) \qquad (7)$$

It was observed during the etching phase of the experiment that water vapor from the oxidation step had condensed in the inlet glassware and was available for pickup by the N_2-O_2 HCl mixture. This would allow reactions (5) through (7) to proceed. The generation of H_2 by (5) and (6) and the reversible nature of (4) probably led to redeposition of polycrystalline silicon around the etch pit, resulting in the observed mound.

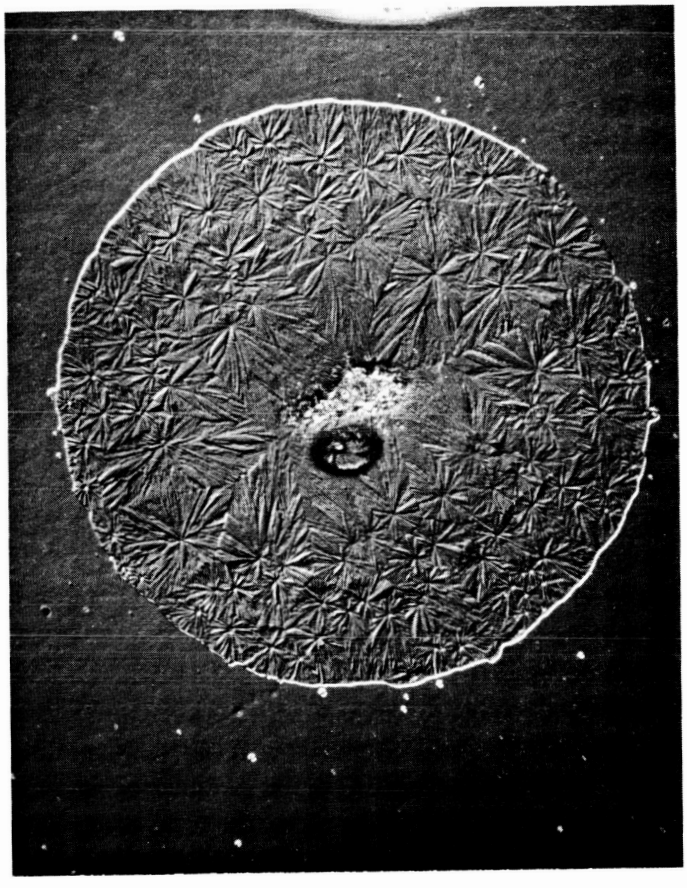

Figure 2. Suspected etch site on wafer No. 6. (125 X)

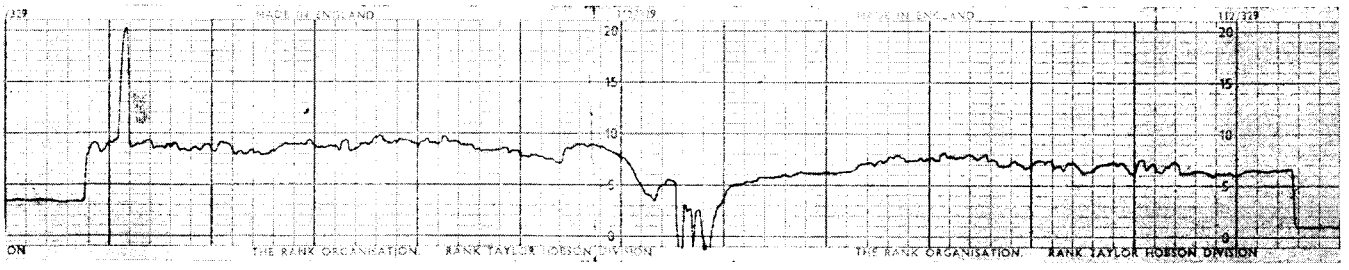

Figure 3. Proficorder trace across region of Figure 2.
(Average mound height: 0.14 microns; Mound diameter: 600 microns.)

It was found, in fact, that with the vapor etching system used the presence of H_2O was necessary to obtain etching. Because of the problems involved in control of H_2O, HCl and carrier gas concentrations a different etching system was adopted using a HCl-He mixture as described by Pinneo and Burk.[7] This system is much more suitable for use in an open tube furnace than a conventional HCl-H_2 mixture since it eliminates the hazards of the possible high temperature H_2-O_2 reaction at the gas outlet point. The following conditions have been shown to produce significant etching.

Temperature	1150 C
He flow rate	13 l/min
HCl flow rate	0.8 l/min
Time	15 min.

Prior to adoption of the vapor etching technique as a defect detection method it was necessary to establish the correlation between decorated defects and etch pits. This was achieved by decorating a number of defects on a wafer and then subjecting the wafer to a vapor etch in an epitaxial reactor using a H_2-HCl mixture.[8,9] A portion of such a decorated wafer is shown in Figure 4. The two decorated regions (1 and 2) are shown in Figures 5 and 6 after the vapor etch. It can be seen that one or more etch pits correspond to each decoration. It was possible to establish this correlation for each decoration. It should be mentioned that the decorations of closely spaced defects often merge and give the appearance of a single defect. During decoration, however, each defect is a source of H_2 bubbles and the count is made at this time to avoid discrepancies.

After establishment of etching conditions with the He-HCl system and verification of coincidence between decoration sites and etch pits, another experiment on etching prior to cooling was performed. Two wafers were inserted in the furnace and oxidized in Steam at 1150 C to an oxide thickness of 5200 Å (determined after removal from the furnace). After the oxidation period the furnace was purged for 40 minutes with dry helium to remove all H_2O from the inlet glassware. An oxidized control wafer which was known to have a number of oxide defects was then inserted into

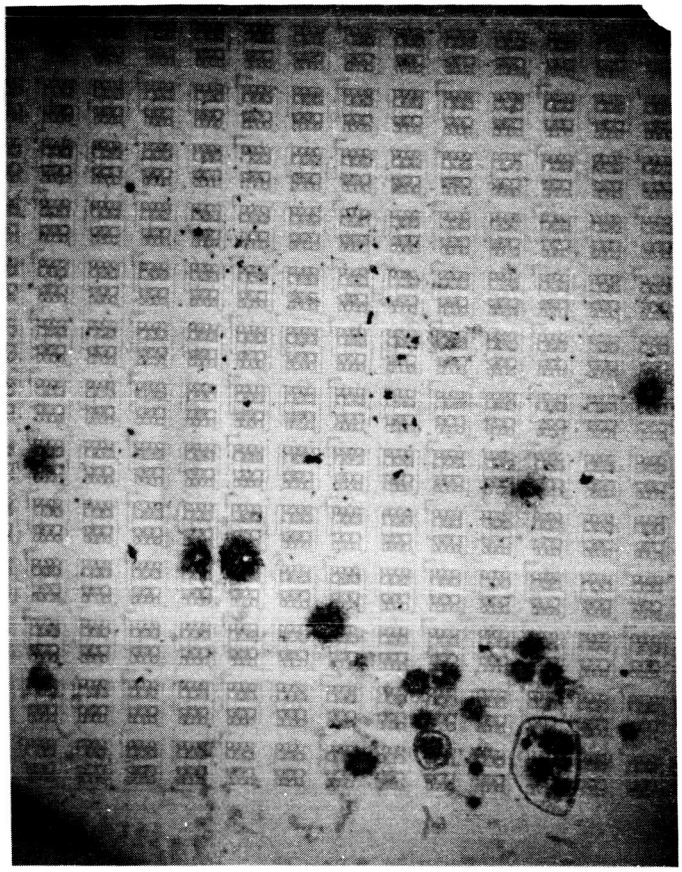

Figure 4. Wafer with oxide defects revealed by decoration. (5X)

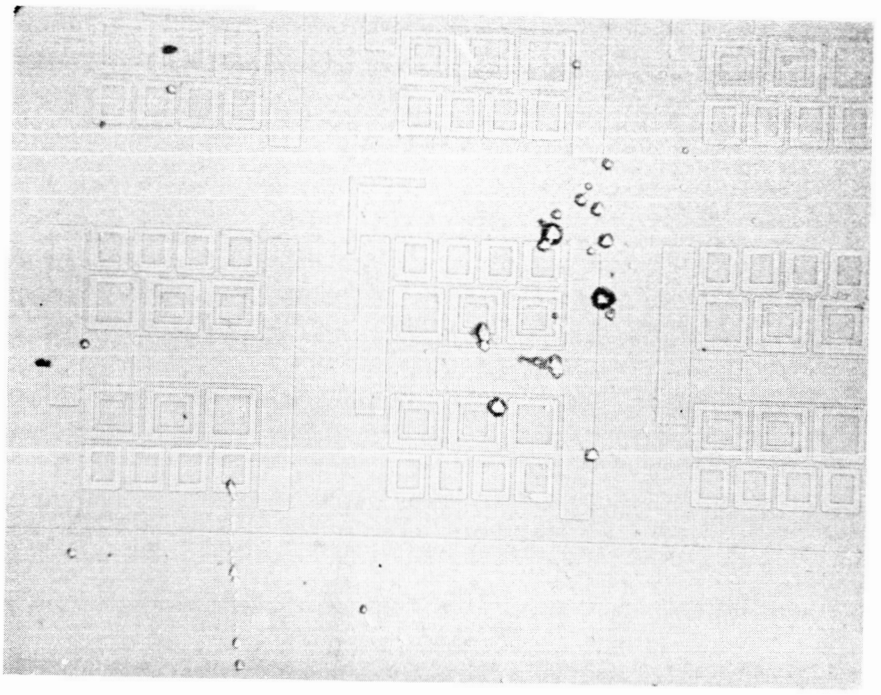

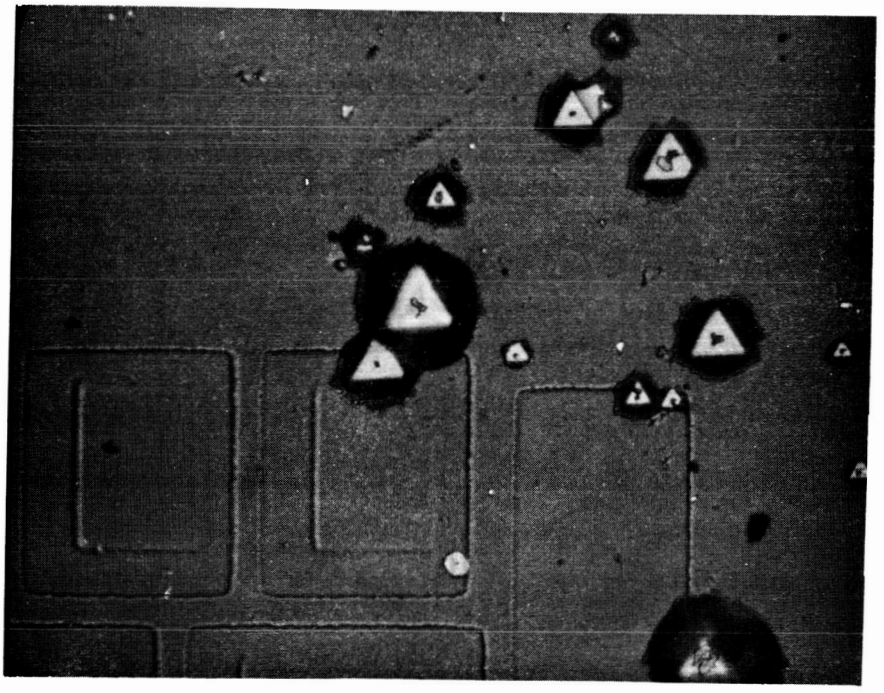

Figure 5. Region 1 of Figure 4 after decoration removed and vapor etch.
a) 35 X b) 175 X

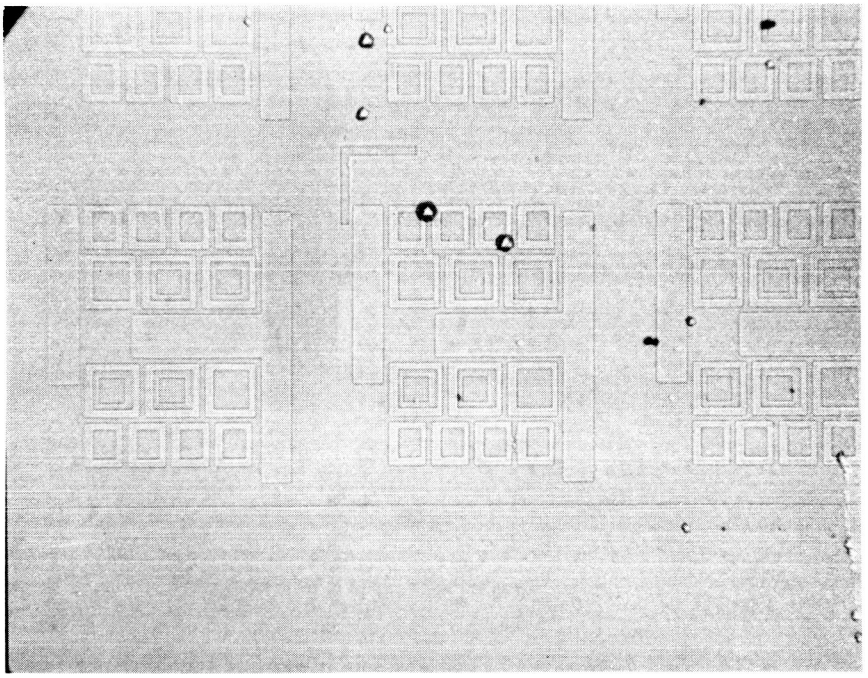

Figure 6. Region 2 of Figure 4 after decoration removal and vapor etch. (35 X)

the furnace and a vapor etch was performed using the He-HCl mixture under the previously described conditions. The HCl flow was terminated and the tube purged with He for 10 minutes. The control sample was removed first and observed to have undergone etching at oxide defect sites. The other two wafers were then removed and found to be free from any etch pits. Subsequent electrophoretic decoration revealed defect densities of 57 cm^{-2} and 50 cm^{-2}, providing additional substantiation of the conclusion that oxides are essentially continuous when grown, and defects originate by rupture upon cooling.

It is evident that the combination of the vapor etching and the decoration technique provides a powerful tool for investigating other hypotheses concerning the effect of process steps on oxide quality, e.g., the ineffectiveness of oxide regrowth, the increase in defects as a result of thermal cycling and the result of oxide removal from one side of the wafer.

The latter falls into the second general area of study and has already been under investigation[9] by means of replicate electron microscopy in conjunction with the decoration technique.

A wafer with the isolation pattern defined was oxidized in steam to produce a backside oxide thickness of 4000 Å. After oxidation a replica of the device surface oxide was made. This oxide was then tested for defects by the decoration method without removing the oxide from the reverse side. Defects in certain areas were photographed and a post-test replica of the device side was made. The backside oxide was then stripped, a replica was made, the decoration test performed, additional and previous defects photographed and a final replica made. A photograph of the central region of the wafer after first decoration is shown in Figure 7 with the two decorated defects circled. Figure 8 is a photograph of the same region after the second decoration test (after back oxide removal). The increase in defects is evident. The three specific defects indicated in Figure 8 have been examined from replicas made at each stage of the experiment. Defect No. 1 was detected with the first decoration while Nos. 2 and 3 were not detected at the first decoration but were present at the second decoration. Figure 9 shows that a rupture was present

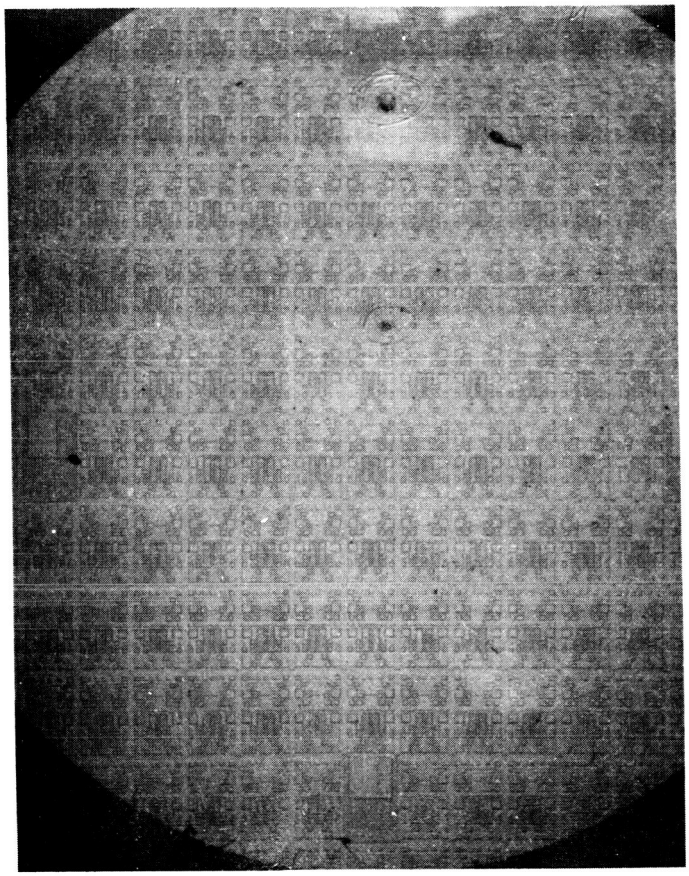

Figure 7. Central region of wafer after decoration with back oxide intact. (5 X)

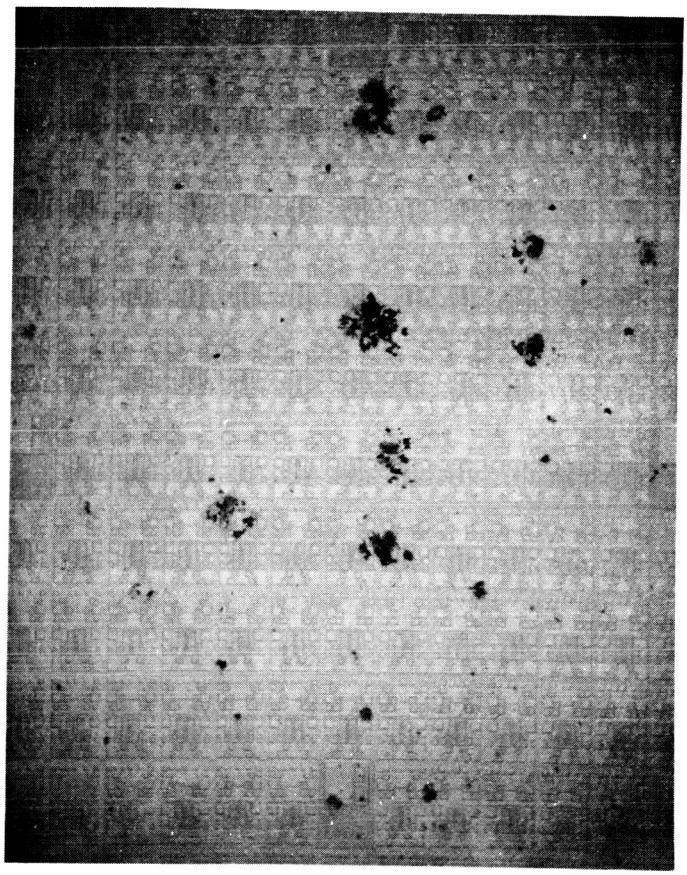

Figure 8. Region of Figure 7 after decoration subsequent to removal of oxide from reverse side. (5 X).

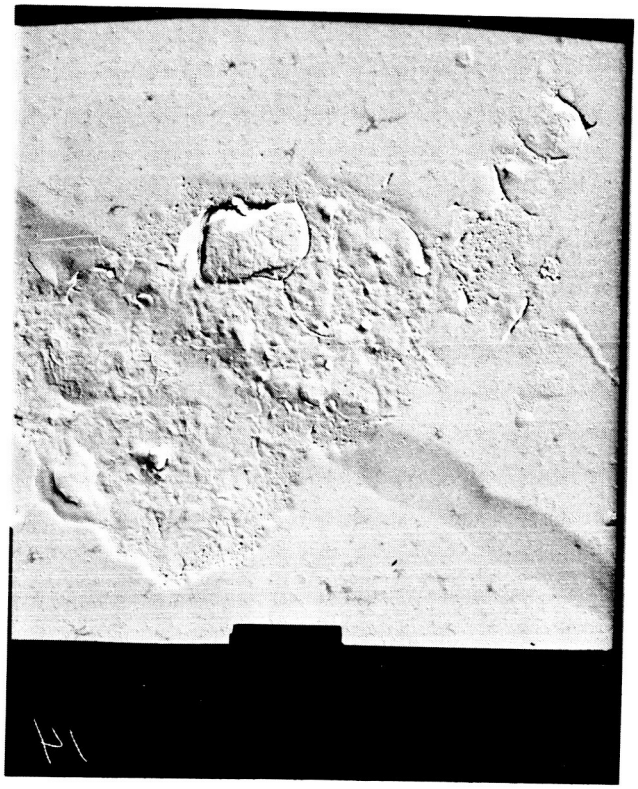

Figure 9. Surface replica of defect No. 1 region before first decoration. (5,000 X)

in the oxide at the location of defect No. 1 before the first decoration. No alteration of the oxide surface occurred as a result of the first decoration and the back oxide removal. (See Figures 10 and 11). After the second decoration considerable damage was observed in the vicinity of the original defect as shown by Figure 12. In the case of defect No. 2, no discernable rupture of the oxide is evident until after the second decoration (Figures 13-16). At the third defect, damage to the oxide by the back oxide removal is observed as shown in Figure 19.

An additional portion of the oxide in this region was subsequently removed by the second decoration. (See Figure 20). In all three cases the first decoration test did not visibly damage the oxide layer. However, considerable damage to the oxide apparently results from the second decoration test. This is interpreted as indicating that the test itself is not detrimental to the oxide. It is concluded that the removal of the oxide from the wafer backside produces structural damage in the bulk of the remaining oxide, which may or may not be manifested in the oxide surface texture. The damaged area, however, apparently presents a lower impedance to current flow and allows passage of charge sufficient to produce, at the Si surface or in the oxide, the hydrogen evolution which occurs in the decoration test. This gas then dislodges a portion of the damaged oxide and produces the alteration observed as a result of the test. This means that the increase in defects observed after backside oxide removal is real and probably results from damage to the oxide caused by flexure of the wafer when its stress profile is altered by this removal.

One significant factor that can be observed in the replicas, (Figures 9 - 20), is that the defects in all three cases occur in a region where a blemish or anomaly is present on the oxide surface. This suggests that these blemishes represent the weak spots in the oxide layer where rupture can most easily occur. The source of these variations in oxide texture is still undetermined and is the basis for the effort in area III. It is considered possible that the substrate-related defects discussed in previous reports manifest themselves as blemishes or variations in the oxide film structure.

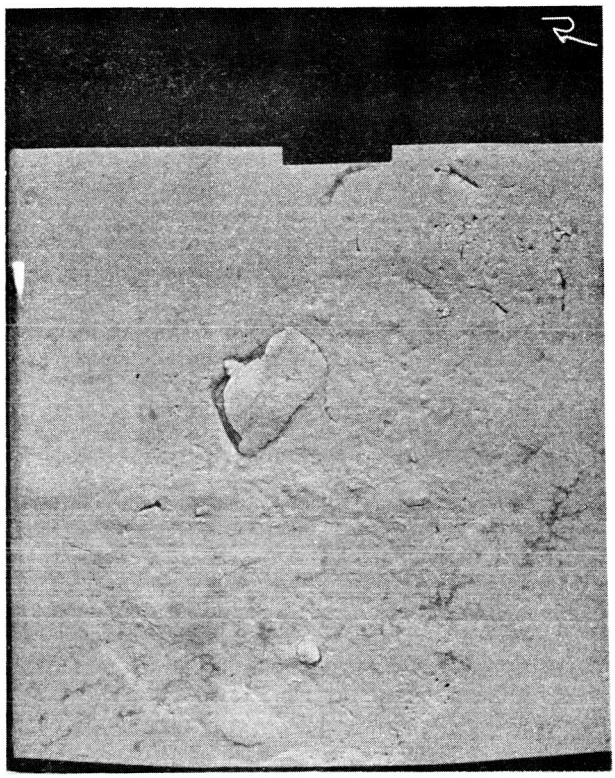

Figure 10. Region of defect No. 1 after first decoration. (5,000 X)

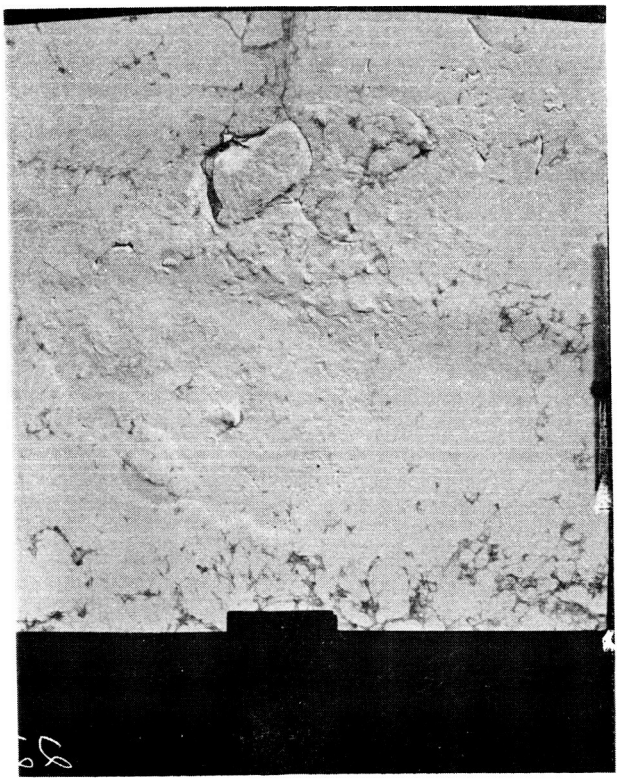

Figure 11. Region of defect No. 1 after backside oxide removal. (5,000 X)

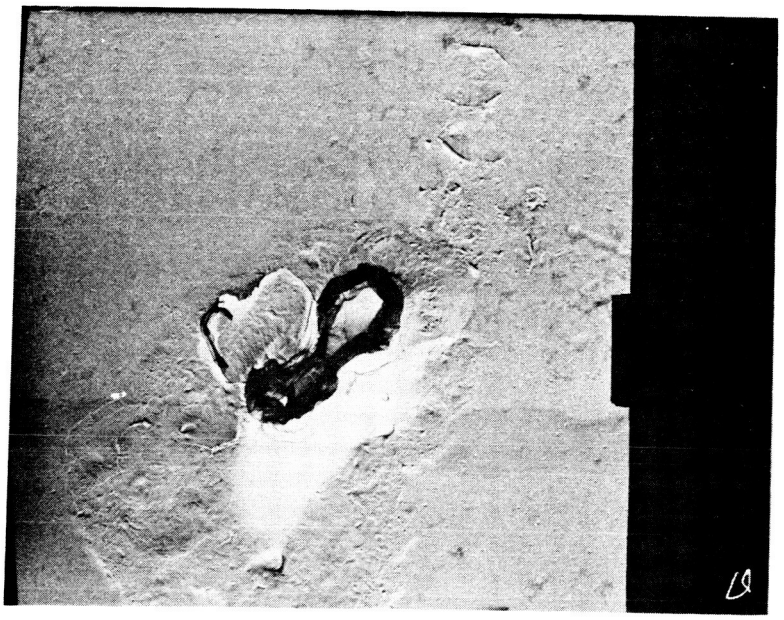

Figure 12. Region of defect No. 1 after second decoration. (5,000 X).

Figure 13. Defect No. 2 before first decoration. (5,000 X)

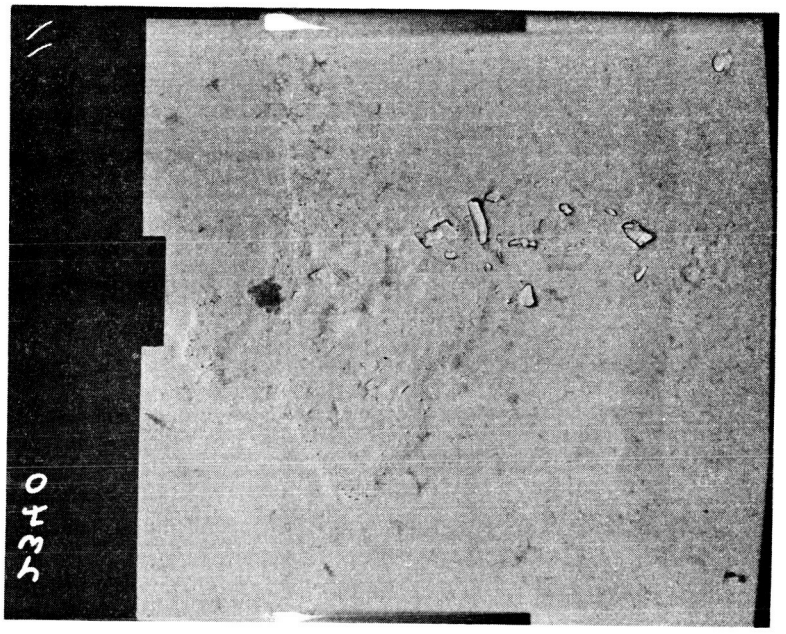

Figure 14. Defect No. 2 after first decoration. (5,000 X)

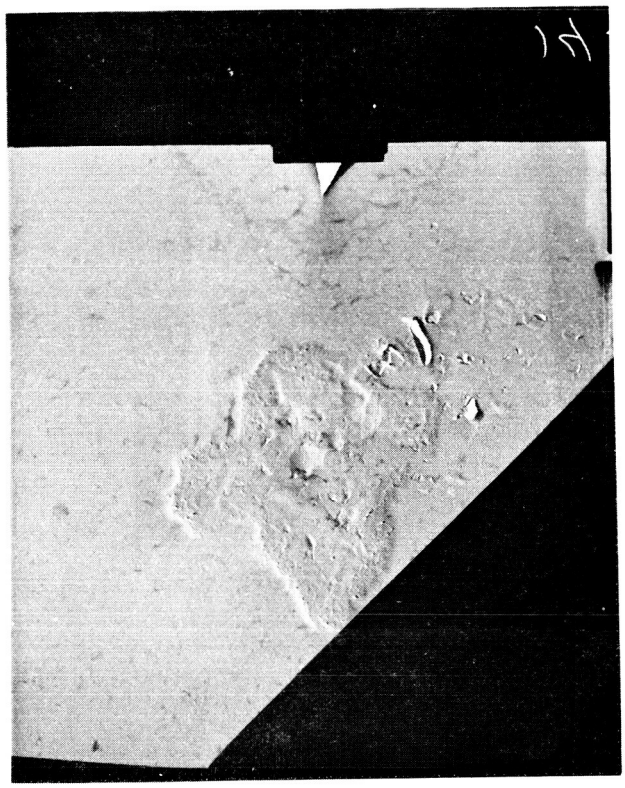

Figure 15. Defect No. 2 after backside oxide removal. (5,000 X)

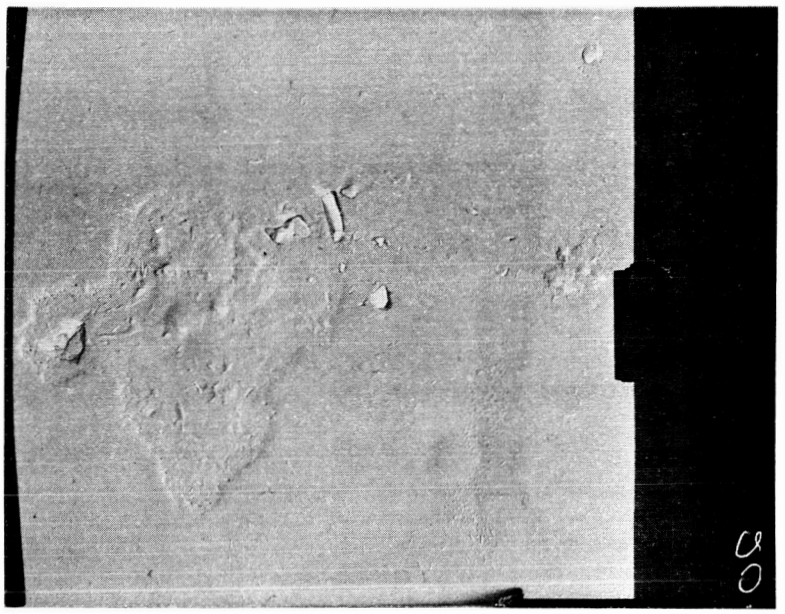

Figure 16. Defect No. 2 after second decoration. (5,000 X).

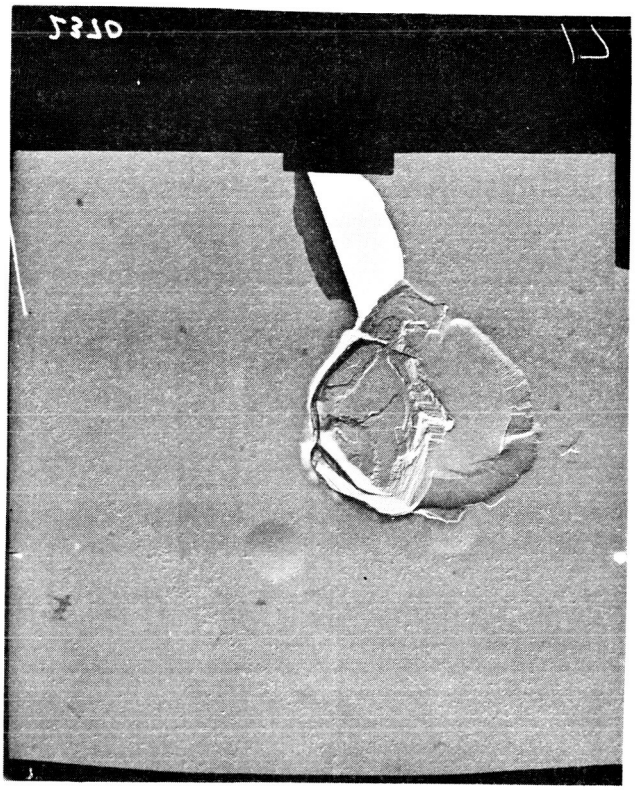

Figure 17. Defect No. 3 before first decoration. (5,000 X)

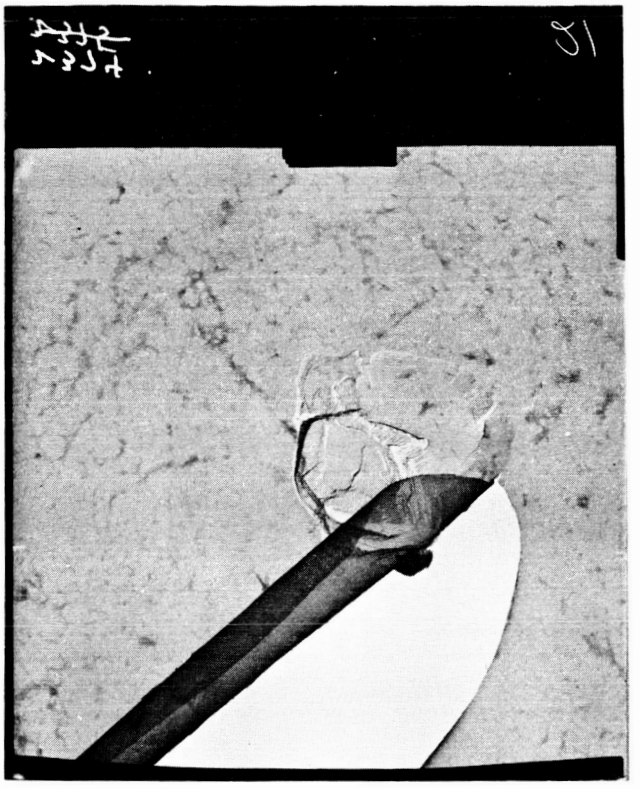

Figure 18. Defect No. 3 after first decoration. (5,000 X)

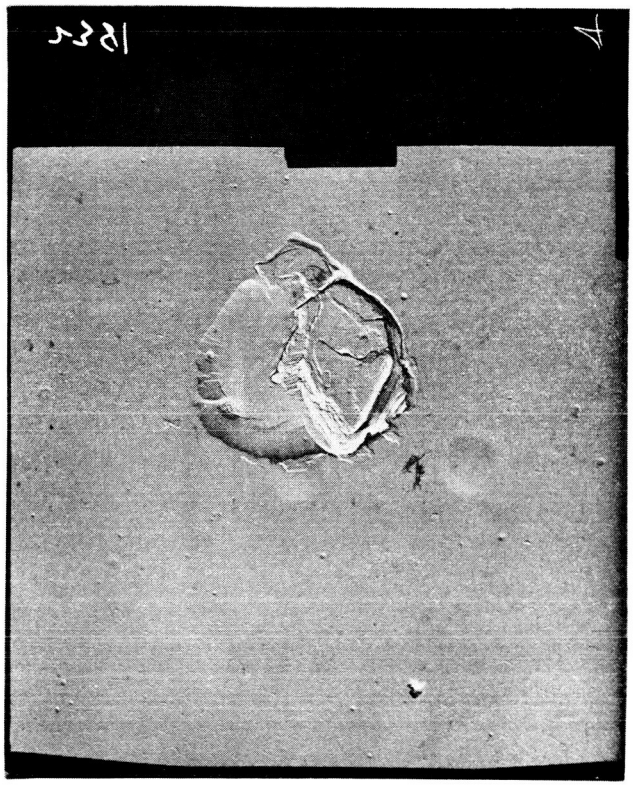

Figure 19. Defect No. 3 after backside oxide removal. (5,000 X).

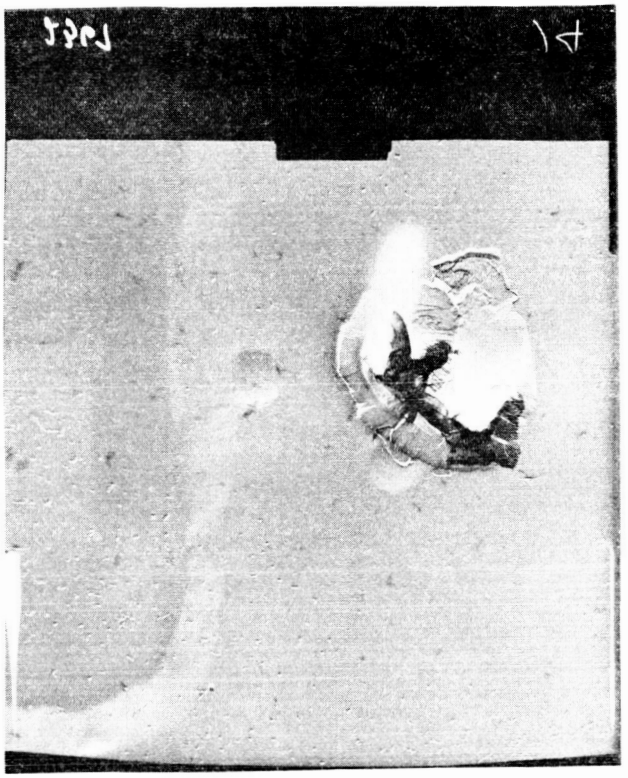

Figure 20. Defect No. 3 after second decoration. (5,000 X).

A number of experiments have been initiated to ascertain the nature of possible substrate defects leading to variations in oxide structure. To investigate the effect of dislocations a comparison was made of defect densities in oxides on Si substrates grown by the Czochralski and float zone methods. The latter technique results in a much higher dislocation density in the Si crystal than does the former. The details and results of the experiment follow.

Material Source	Texas Inst (CZ)	Dow Corning (FZ)
Resistivity Range -	16 - 24 ohm-cm	85 - 93 ohm-cm
Dopant -	Phosphorus	Phosphorus
Orientation -	(111)	(111)
Area of Wafer (cm^{-2})	5.07	5.07

Two wafers from each group were oxidized under the following conditions:

Thickness -	3800 A
Growing time -	12 hrs.
Dry Nitrogen -	1.0 unit @ 2.5 psi
Dry Oxygen -	1.0 unit @ 2.5 psi
Furnace Temp.	1150 C

The back oxides were removed with HF and the defects decorated, yielding the following results:

	TI	TI	DOW	DOW
Defects	109	129	250	265
Densities (cm^{-2})	22	25	49	52

Two wafers from each group were oxidized under the following conditions:

Thickness -	4200 A
Growing time -	25 min
Dry Nitrogen -	1.0 unit @ 2.5 psi
Dry Oxygen -	1.0 unit @ 2.5 psi
H_2O Temp.	100 C
Furnace Temp.	1150 C

Decoration after removal of the back oxides gave the following results:

	TI	TI	DOW	DOW
Defects	75	80	151	145
Densities (cm^{-2})	14	16	30	29

It can be seen that the defect density is higher by a factor of approximately 2 in the oxides grown on float zone material. The dislocation density is higher by a considerably greater factor but it may be possible that only certain types or groupings of dislocations result in oxide defects (i.e., not every dislocation produces a defect) or that there are many more latent defects in the float zone sample that may rupture on further thermal cycling.

To investigate the latter possibility, the 8 wafers were subjected to a thermal cycle consisting of heating at 1150 C for 5 minutes in N_2 and recooling to room temperature. The decoration test was performed again with the following results:

DEFECT DENSITIES (cm^{-2})

Grown Wet

	TI	TI	DOW	DOW
Original	14	16	30	29
After Cycle	43	53	51	58

Grown Dry

	TI	TI	DOW	DOW
Original	25	22	49	52
After Cycle	112	88	127	115

This indicates that the oxides on the Czochralski substrates had more latent defects than those on the float zone substrates in contradiction to expectation if a strong correlation existed between dislocations and oxide anomalies. After one thermal cycle all wafers have essentially the same defect density. It appears doubtful on the basis of these results, that silicon dislocations can be identified as a major source of oxide dielectric defects.

Another experiment consisted of growing oxides on epitaxial Si layers with varying stacking fault densities (from ~ 100 cm^{-2} to $\sim$ 10,000 cm^{-2}). The samples were oxidized in steam at 1150 C producing oxides 3700 Å thick. Defect densities were measured before and after back oxide removal. No significant defect density difference was observed on wafers with different stacking fault densities.

The results of this experiment indicate that stacking faults are not a type of substrate defect which is responsible for the incidence of oxide dielectric defects.

Since the sample on which the replicate electron microscopy was performed is still intact, it is planned to examine the substrate beneath the three oxide defects in the hope of obtaining some insight into the nature of possible substrate origins of oxide variations.

It is concluded that defects in oxide layers originate during cooling from high temperature treatments probably as a result of thermal expansion mismatch; that all treatments that cause flexing of the wafer, such as back oxide removal, introduce additional defects; and that the occurrence of dislocations or stacking faults in the substrate silicon is unrelated to the generation of oxide defects.

PROPOSED PLAN FOR FOLLOWING QUARTER

Investigation of tritium beta assay technique will be continued. Additional investigation of proton electromigration and exchange with sodium will be made.

Gas ambient investigations will be resumed.

EPR experiments will be summarized and correlated with process variables.

Oxide defect investigations will continue with emphasis on morphological characterization by electron microscopy, further correlation with oxide regrowth and back oxide removal, and structural modifications aimed at reducing mismatch in thermal properties.

COMPLETION INFORMATION

Approximate physical completion (current year)	72%
Approximate expenditures	69%

ACTION REQUIRED BY NASA

None

ACKNOWLEDGEMENTS

Contributions to the work reported herein were made by P. J. Besser, J. V. Brandewie, K. J. Brion, R. Cunningham, T. E. Hagey, R. L. Nolder, C. W. Scott, G. Shaw, and R. D. Yurges.

REFERENCES

1. T. E. Burgess and F. M. Fowkes, Electrochemical Society Spring Meeting, 1966; Extended Abstracts, Electronics Division 15, No. 1, 110 (1966).

2. P. J. Burkhardt, J. Electrochem. Soc. 114, 196 (1967); Electrochemical Society Spring Meeting, 1966, Recent News Paper No. 18.

3. Chung and Haneman, J. Appl. Phys. 37, 1879 (1966)

4. P. J. Burkhardt, IEEE Transactions on Electron Devices ED-13, No. 12, 268 (1966).

5. G. Feher and A. F. Kip, Phys. Rev. 98, 337 (1955).

6. T. L. Chu and R. L. Tallman, J. Electrochem. Soc. 111, 1306 (1964).

7. G. G. Pinneo and P. E. Burk, Extended Abstracts, Electronics Division of the Electrochemical Society 15, No. 2, Abstract 185 (1966).

8. The assistance of Mr. G. Shaw in performing the H_2-HCl etching and establishing the conditions for the He-HCl system is greatly appreciated.

9. Twentieth Monthly Report, December, 1966, p. 10